KRYSTYNA GADZINOWSKA, EWA PIORKOWSKA

Centre of Molecular and Macromolecular Studies
Polish Academy of Sciences,
ul. Sienkiewicza 112, 90-363 Łódź, Poland
e-mail: epiorkow@bilbo.cbmm.lodz.pl

Influence of sample thickness and surface nucleation on *i*-PP crystallization kinetics in DSC measurements

Summary — The crystallization of isotactic polypropylene was studied by DSC method at a standard cooling rate of 10 deg/min. The samples were in the forms of sandwiches comprising polymer films of various thickness and layers of foreign materials. After the crystallization the spherulitic structure of the samples was investigated in thin transversal sections by light microscopy. DSC crystallization peak positions depend on the type of the interface and the sample thickness. The weak spherulite nucleation was found at interfaces of polypropylene with constantan, polystyrene, aluminum, nickel and mica, while poly(tetrafluoroethylene) and polyimide films revealed intense nucleation activity leading to transcrystallinity. The DCS curves are interpreted with a help of the developed earlier probabilistic model of spherulitic structure formation.

Key words: crystallization, modeling, isotactic polypropylene, differential scanning calorymetry, sample thickness, nucleation of spherulites.

Polymers solidify frequently in contact with foreign surfaces, which dependent on their nucleation ability can influence both the kinetics of crystallization and the spherulitic pattern. The conversion of melt into spherulites in such conditions was mathematically modeled and computer simulated [1—4]. It is already known that the spatial limits slow down the crystallization when limiting surfaces do not nucleate spherulites. Spherulitic nucleation on those surfaces accelerates the solidification and, in the case of transcrystallinity, may even lead to a change in shape of the conversion rate curve.

Recently, Billon *et al.* [5, 6] demonstrated that transcrystallinity originating from the contact surface of high density polyethylene sample with DSC pan could significantly influence the crystallization kinetics and lead to buildup of a shoulder on DSC peak. The effect was enhanced at small sample thickness and slow cooling. The method of extracting the kinetics data for both the polymer crystallization inside a sample and the transcrystallinity are proposed in ref. [6], requiring however, the DSC measurements at various sample thickness and cooling rates.

The contact with aluminum DSC pan may not lead to the transcrystallinity development in polymers other than polyethylene. On the other hand it was predicted in ref. [4] that even rather weak spherulite nucleation on sample surfaces could affect the conversion rate of melt

into spherulites, although it did not lead to buildup of the shoulder on DCS peak.

Our studies concern the crystallization and the structure of isotactic polypropylene (*i*-PP) samples of various thickness crystallizing in the contact with the other materials. The results were interpreted with the help of the model developed earlier by Piorkowska [3, 4], allowing to account for the influence of both the spatial limits and the spherulite nucleation on the kinetics of spherulitic crystallization.

EXPERIMENTAL

Materials

i-PP (Rapra) ($M_w = 307\,000$, $M_w/M_n = 20$, density 0.906 g/cm^3, melt flow index (*MFI*) 3.9 g/10 min) was used in the studies. Films of thickness approximately 280±15, 90±10 and 45±5 μm were obtained by compression moulding at 190 °C. Prior to encapsulating in DSC standard aluminum pans, circles of 5 mm diameter, cut out from *i*-PP films, were placed between circles of foils of different materials.

The polymers: poly(tetrafluoroethylene) (PTFE), polyimide (PI) (Kapton, DuPont product), and atactic polystyrene (*a*-PS) manufactured by Polysciences Inc. were used. The respectively low molecular weight *a*-PS,
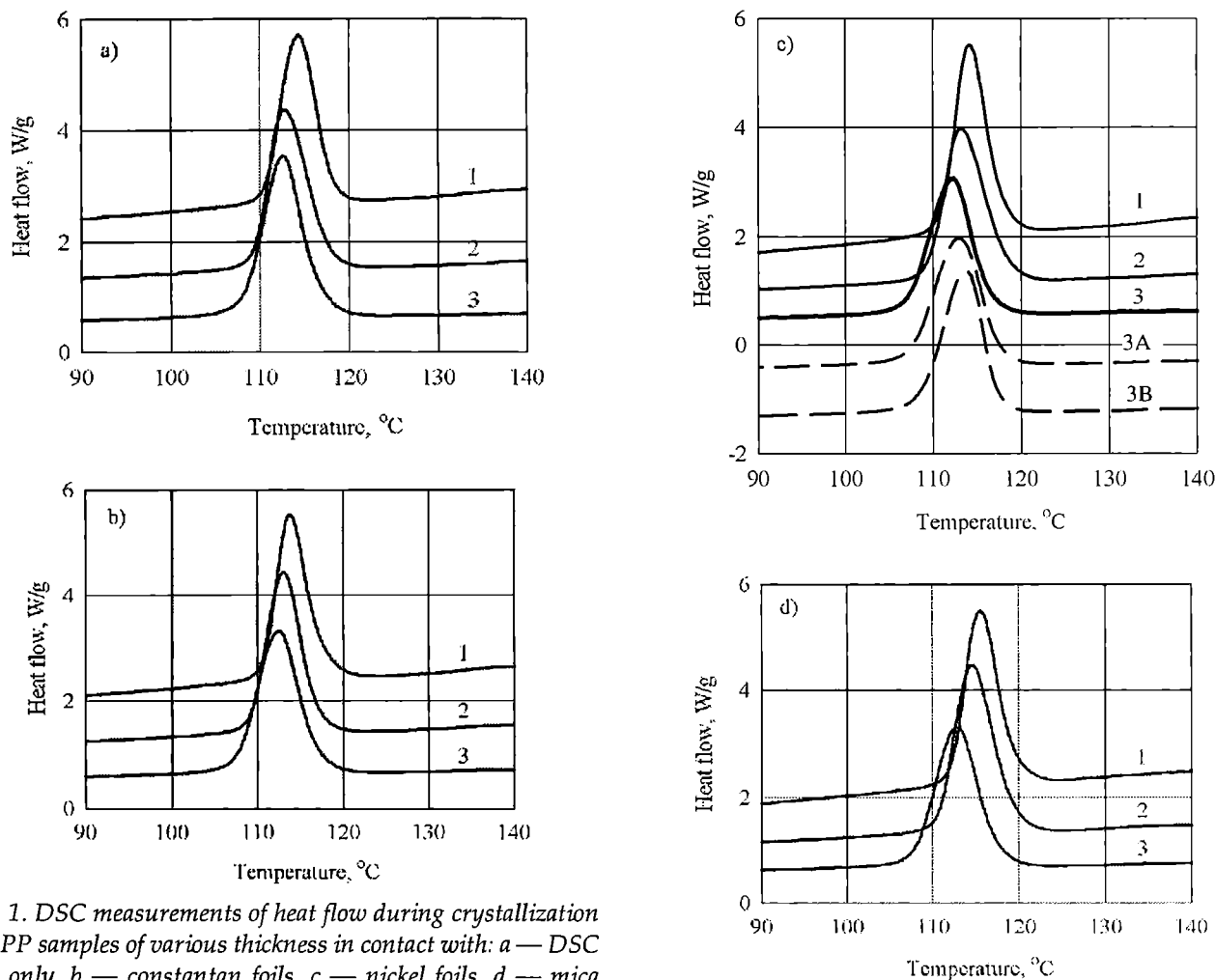
Fig. 1. DSC measurements of heat flow during crystallization of i-PP samples of various thickness in contact with: a — DSC pan only, b — constantan foils, c — nickel foils, d — mica plates; total thickness of i-PP layers in μm: 1 — 45, 2 — 90, 3 — 280; dashed lines denote multilayered sandwiches: A — 3 layers, B — 6 layers. Curves are shifted along the vertical axis for clarity

of M_w = 20 000, and showing T_g about 50 °C, was selected in order to have a liquid-liquid interface during i-PP crystallization.

The other materials were mica and metals: constantan and nickel (Ni).

The thickness of a single layers of those materials was: 125 μm — PTFE, 25 μm — PI, 45 μm — a-PS, 22 μm — mica and 8 μm — metal foil. In addition, the sandwiches comprising alternating layers of i-PP and a spacer were prepared for i-PP-PI and i-PP-Ni systems. In these sandwiches the total thickness of 3 and 6 i-PP layers was approximately 280 μm.

The i-PP samples of various thickness without any foreign material were also studied, thus i-PP was in contact only with DSC standard aluminum pan. In this case 280 μm thick samples were directly cut out from the film of respective thickness. In order to check whether foreign particles able to nucleate i-PP crystallization were not introduced onto film surfaces during film preparation, the 280 μm thick stacks of thinner films were also studied.

Measurements

DSC measurements were performed using TA Instruments DSC 2920. Samples were melted, annealed at 220 °C for 5 min and cooled down at a rate 10 deg/min. The entire process was carried out under a flow of dry gaseous N_2 to prevent the degradation. Several samples of each type were examined. After crystallization the samples were microtomed to obtain 10 μm thick sections, which were examined by polarized light microscopy.

EXPERIMENTAL RESULTS AND DISCUSSION

The crystallization curves recorded for 280 μm thick i-PP samples without spacers, independently whether they were cut out from a single film or obtained by stacking of thinner films, were nearly the same, within the limits of experimental error in maximum position not exceeding 1.5 deg. This enabled a conclusion that no significant amount of heterogeneous seeds was introduced onto the polymer surfaces during the films preparation.

Exemplary DSC curves recorded for the films of i-PP crystallizing in contact with other materials are plotted

in Figures 1 and 2. In all cases the integration of peaks gives nearly the same values of heat of i-PP crystallization equal to 106±3 J/g. The average values of the temperature of maxima for all systems studied are collected in Table 1.

T a b l e 1. Average values of the temperature of DSC curve maxima recorded during i-PP crystallization in contact with foreign materials. Asterisk denotes multilayered systems

| Spacer | Temperature of maximum, °C | | |
	Total i-PP layer thickness, μm		
	280	90	45
None	111.8	112.7	114.2
Constantan	111.6	113.2	113.6
Ni	112.0	113.5	114.0
Ni, 3 i-PP layers*	112.9	—	—
Ni, 6 i-PP layers*	113.7	—	—
Mica	111.7	114.1	115.2
a-PS	111.7	112.5	113.4
PI	112.2	114.9	117.8
PI, 3 i-PP layers*	114.3	—	—
PI, 6 i-PP layers*	116.7	—	—
PTFE	112.4	114.6	117.8

The temperature of DSC curve maximum recorded for i-PP film in contact with foreign substance changes insignificantly in the case of 280 μm thick samples. The maxima of DSC peaks for systems i-PP-a-PS (Fig. 2a), i-PP-mica (Fig. 1d) and i-PP in contact with metals (Fig. 1a—c) shift up to 2.5 deg towards the higher temperature with the decrease in sample thickness. This effect is accompanied with slight narrowing of the peaks. As it is seen in Figs. 2b and 2c the DSC curves recorded for i-PP-PI and i-PP-PTFE systems start to rise at a higher temperature than those for other systems. In the case of 280 μm thick samples noticeable deviation from the baseline is observed before the build-up of the peaks. The lower parts of the low temperature slopes of the peaks for all 280 μm thick i-PP samples are similar, independently on the contacting material, indicating comparable kinetics of late stage of crystallization. With the decrease in i-PP sample thickness in i-PP-PI and i-PP--PTFE systems the maxima of DSC curves shift significantly to higher temperature, up to 5.5 deg. Although the signal begins to rise at the same temperature as for 280 μm thick samples, the peaks are steeper and decline sharply after reaching the maximum value. The observed changes are more visible for the samples of i-PP--PTFE system. On the high temperature slopes of DSC peaks for 45 and 90 μm thick samples of this system the traces of shoulders can be recognized.

The results obtained for i-PP-Ni (Fig. 1c) and i-PP-PI (Fig. 2b) sandwiches also show the elevation of maximum temperature with the decrease in i-PP sample layer thickness, and the obtained values are only slightly
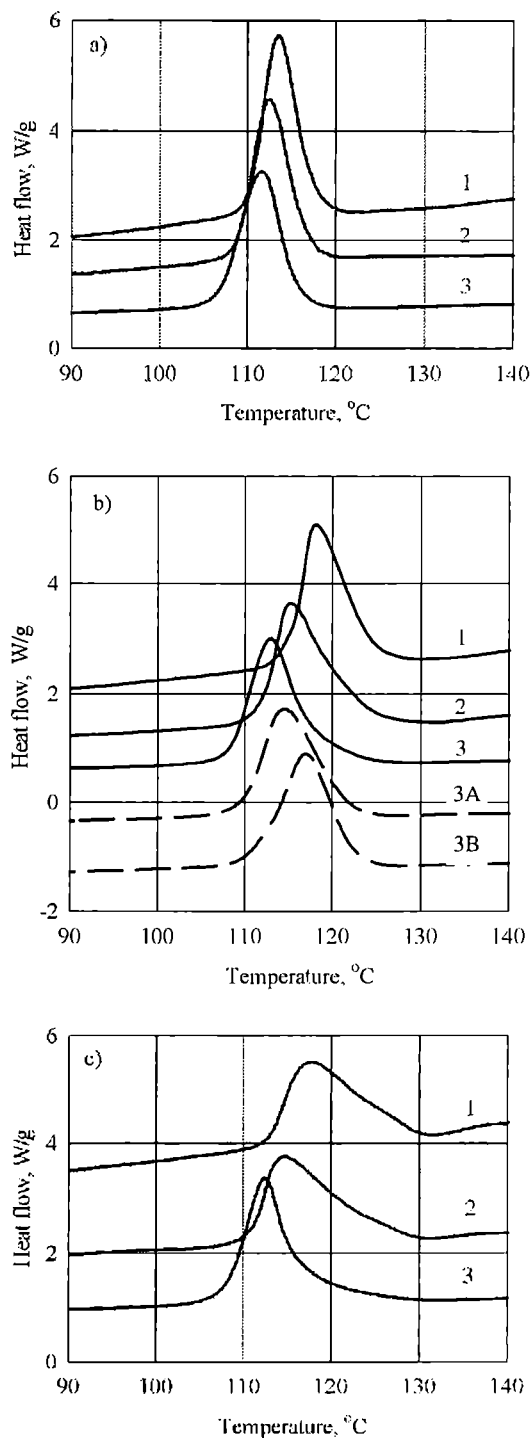
Fig. 2. DSC measurements of heat flow during crystallization of i-PP samples of various thickness in contact with: a — a-PS layers, b — PI films, c — PTFE films; curves denotations — see Fig. 1. Curves are shifted along the vertical axis for clarity

higher than those measured for single i-PP samples in respective systems.

The exemplary micrographs of spherulitic structure in i-PP samples crystallized in DSC cell are shown in Figs. 3—5. As it follows from polarized light microscopy all samples contain predominantly spherulites of α crystallographic form. The spherulites nucleated inside
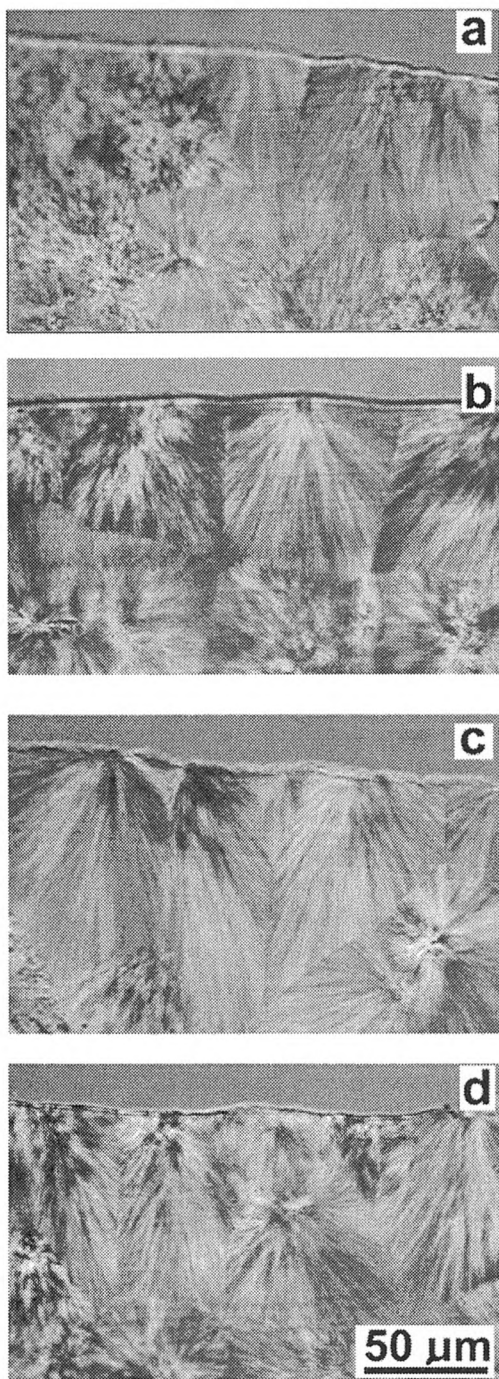
Fig. 3. Polarized light micrographs of sections of i-PP samples of thickness 280 µm, crystallized in DSC apparatus in contact with: a — constantan foils, b — DSC pan (Al), c — nickel foils, d — mica plates

Fig. 4. Polarized light micrographs of sections of i-PP samples of thickness 280 µm, crystallized in DSC apparatus in contact with: a — a-PS layers, b — PI films, c — PTFE films

280 µm thick samples visible on several micrographs were counted and the average spherulite area was calculated as equal to 3400 µm².

The studies of thin sections of i-PP films have shown the weak nucleation of i-PP spherulites at the interfaces with constantan, a-PS, Ni, Al and mica. Weak nucleation of i-PP spherulites on the interfaces with a-PS was also reported previously in ref. [7]. The boundaries betw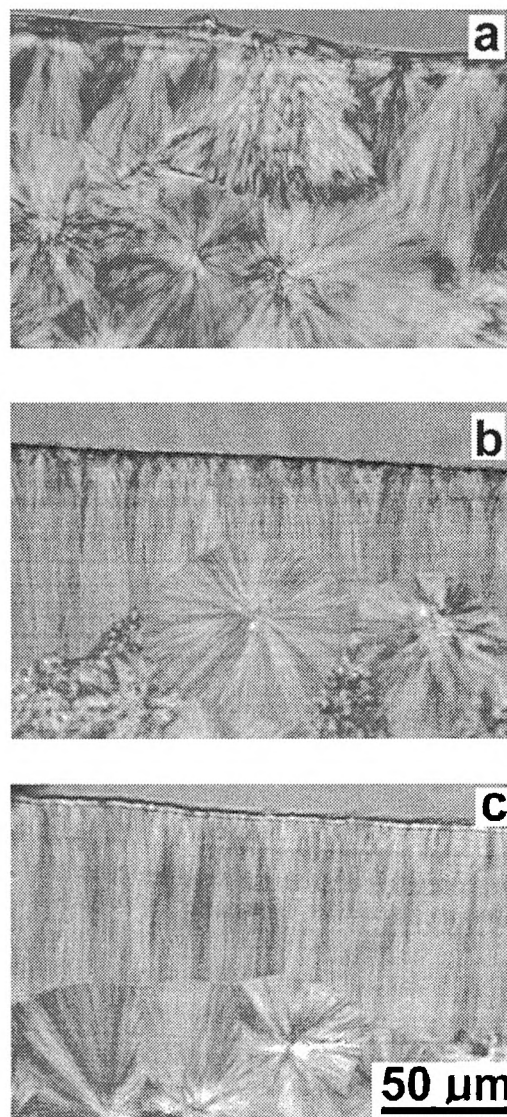een spherulites nucleated inside i-PP are curved, indicating that not all spherulites started to grow at the same time. The boundaries between spherulites nucleated on sample surfaces in those systems do not show any significant curvature indicating that those spherulites were nucleated within a short time interval. Very strong nucleation, resulting in transcrystallinity, was found on i-PP surfaces adhering to PI and PTFE. While spherulites nucleated inside i-PP are seen in 280 µm thick samples crystallizing in contact with these polymers, they practically disappear in the thinner samples. The thinner samples are predominantly filled with transcrystalline layers originating from the sample surfaces.

The results obtained clearly indicate the influence of the spherulite nucleation on the sample surfaces and the sample thickness on the kinetics of conversion of a melt into spherulites, reflected in a heat flow recorded during the nonisothermal crystallization in the DSC apparatus. The maximum of DSC crystallization peak can be shifted
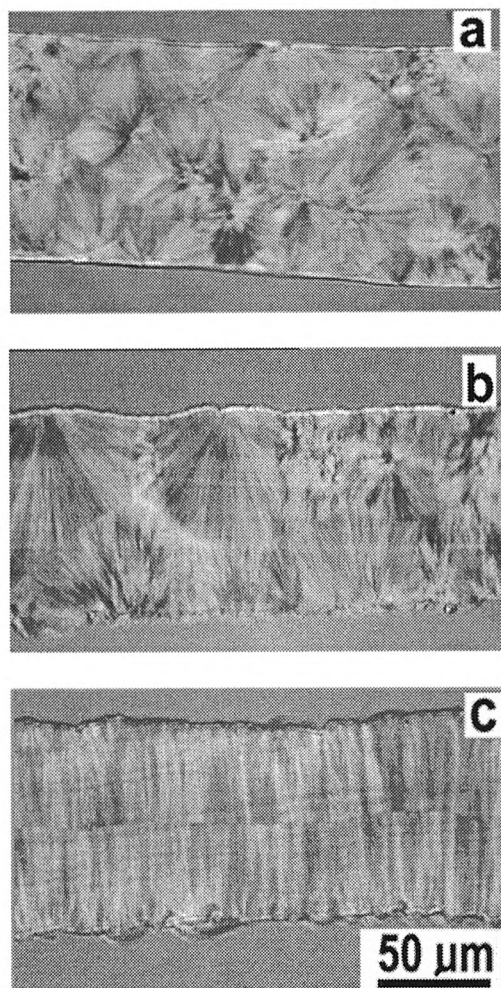
Fig. 5. Polarized light micrographs of sections of i-PP samples of thickness 90 μm, crystallized in DSC apparatus in contact with: a — constantan foils, b — nickel foils, c — PTFE films

as much as 5.5 deg depending on the sample thickness and the material being in contact with sample surface.

MODELING

Model

To explain the changes of the positions of DSC peaks during crystallization of i-PP films, the model elaborated previously for a crystallization in confined volume [3, 4] was used. In this model the spherulite growth rate (G), and nucleation rate both inside a polymer matrix (F), and on the sample surfaces (F_s), are treated as dependent on time. The conversion rate (Q) of the crystallization in a plate of thickness 2h, at time t, depends on the distances between sample surfaces, s and 2h-s [eqn (1)]. In further text the symbols with an asterisk at superscript represents the dependence on time while missing asterisk represents the dependence on temperature. This difference concerns quantities which may be expressed as functions of either time temperature.

$$Q^*(t, s, 2h-s) = \frac{\delta\left[E^*(t, s, 2h-s)\right]}{\delta t} \exp\left[-E^*(t, s, 2h-s)\right] \tag{1}$$

$$E^*(t, s, 2h-s) = E_\infty^*(t) - H^*(t, s) + H_s^*(t, s) - H^*(t, 2h-s) + H_s^*(t, 2h-s) \tag{2}$$

$$r(t', t) = \int_{t'}^{t} G^*(\tau)d\tau \tag{3}$$

where: $r(t', t)$ is the integral of the time dependence of the growth rate G^* over time range (t', t); E_∞^* has the same form as for infinite sample; $H^*(t, s)$, [being non zero for $r(0, t) > s$] and $H^*(t, 2h-s)$ [being non zero for $r(0, t) > 2h-s$] describe the influence of the first and the second plate surfaces, at distances s and $2h-s$ from the considered point, when no additional spherulite nucleation occurs on those surfaces, the terms $H_s^*(t, s)$ [being non zero for $r(0, t) > s$] and $H_s^*(t, 2h-s)$ [being non zero for $r(0, t) > 2h-s$], describe the influence of the additional nucleation process on the local conversion.

For instantaneous nucleation on sample surfaces, of the density D_s, the functions assume the forms:

$$E_\infty^*(t) = \left(\frac{4}{3}\right)\int_0^t F(t')\pi[r(t', t)]^3 dt' \tag{4}$$

$$H^*(t, s) = \pi\int_0^{t_k} \frac{F(t')\left\{s^3 + 2[r(t', t)]^3 - 3[r(t', t)]^2 s\right\}}{3} dt' \tag{5}$$

$$H_s^*(t, s) = \pi\int_0^{t_k} F_s(t')\left\{[r(t', t)]^2 - s^2\right\} dt' \tag{6}$$

where: t_k is defined by the relation $r(t_k, t) = s$.

For a constant cooling rate, temperature can be easily substituted for time. We have to note that during non-isothermal crystallization the growth rate depends on momentary temperature, while the nucleation rate depends on temperature, time and polymer thermal history. Not knowing the exact dependence of nucleation rate in i-PP studied we assume an instantaneous nucleation in i-PP characterized by the density D, being aware that this might be a potential source of discrepancies. From the experimental results it follows that the spherulite nucleation on sample surfaces being in contact with metals, mica and aPS occurred within a short time interval. Thus the nucleation process can be treated as instantaneous and for a given system and cooling experiment it can be characterized by the density D_s, being the number of primary nuclei per unit area of the surface. Although the interspherulitic boundaries in transcrystalline layers originating from the sample surfaces being in contact with poly(tetrafluoroethylene) or polyimide are not clearly recognizable, we assume that they result also from an instantaneous nucleation. The nucleation process on the sample surfaces can occur either before the nucleation inside a polymer matrix or at the same time. Hence, the eqs. 3—6, expressed in the form of temperature dependencies, assume the form:

$$E(T, T_i, T_s, s, 2h-s) = E_\infty(T_i, T) - H(T_i, T, s) + H_s(T_s, T, s) +$$
$$- H(T_i, T, 2h-s) + H_s(T_s, T, 2h-s) \qquad (7)$$

$$E_\infty(T_i, T) = \left(\frac{4}{3}\right) D\pi [r(T_i, T)]^3 \qquad (8)$$

$$H(T_i, T, s) = \left(\frac{\pi}{3}\right) D \left\{ s^3 + 2[r(T_i, T)]^3 - 3[r(T_i, T)]^2 s \right\} \qquad (9)$$

$$H_s(T_s, T, s) = D_s \pi \left\{ [r(T_s, T)]^2 - s^2 \right\} \qquad (10)$$

where: T_i and T_s denote respectively the temperature at which the nucleation processes inside the polymer and on the sample surfaces occur. $r(T', T)$ [being non zero for $T > T'$] for temperature decreasing from initial value T_0 at a rate v, $T=T_0-vt$, is in the following form:

$$r(T', T) = \left| v^{-1} \int_{T'}^{T} G(T) dT \right| \qquad (11)$$

Besides the cases where $r(T', T)$ equals zero, the functions $H(T_i, T, s)$ and $H_s(T_s, T, s)$ assume a value of zero for $r(T_i, T) < s$ and $r(T_s, T) < s$, respectively.

To obtain the average conversion rate for entire plate the integration has to be performed:

$$Q_{av}(T, T_i, T_s, 2h) = \left| vh^{-1} \int_0^h \frac{\delta [E(T, T_i, T_s, s, 2h-s)]}{\delta T} \cdot \right.$$
$$\left. \cdot \exp[-E(T, T_i, T_s, s, 2h-s)] ds \right| \qquad (12)$$

Following the derivation described in details in [3] it is possible to distinguish two components in the conversion rate: one originating from spherulites nucleated inside the polymer, Q_{iav}, and another one originating from the spherulites nucleated on the surface, Q_{sav}:

$$Q_{iav}(T, T_i, T_s, 2h) = \left| vh^{-1} \int_0^h \frac{\delta [E_\infty(T_i, T) - H(T_i, T, s) - H(T_i, T, 2h-s)]}{\delta T} \cdot \right.$$
$$\left. \cdot \exp[-E(T, T_i, T_s, s, 2h-s)] ds \right| \qquad (13)$$

$$Q_{sav}(T, T_i, T_s, 2h) = \left| vh^{-1} \int_0^h \frac{\delta [H_s(T_s, T, s) + H_s(T_s, T, 2h-s)]}{\delta T} \cdot \right.$$
$$\left. \cdot \exp[-E(T, T_i, T_s, s, 2h-s)] ds \right| \qquad (14)$$

The integration of Q_{iav} and Q_{sav} over time leads to the fractional contents of both spherulite populations in the sample.

Isotactic polypropylene crystallization

The growth rate temperature dependence of α form spherulites of i-PP (Rapra), the same grade as used by

us, in regime III [8, 9] is described by the following formula:

$$G(T) = G_0 \exp \left\{ -U [R(T - T_\infty)]^{-1} \right\} \exp \left\{ -K_g \left[T \left(T_m^0 - T \right) \right]^{-1} \right\} \qquad (15)$$

where: $G_0 = 8009 \, cm/sec$, $U = 1500 \, cal/mol$, $K_g = 358\,400 \, K^2$, $T_\infty = 231.2 \, K$, $T_m^0 = 458.2 \, K$.

The average spherulite area measured in the cross-sections of i-PP samples crystallized in DSC apparatus during cooling at a rate of 10 deg/min was about 3400 μm^2, which is in agreement with the value determined in ref. [10]. It is demonstrated in Appendix I that this corresponds to nucleation density of $2.9 \cdot 10^{-6} \, \mu m^{-3}$. The temperature of 130 °C was chosen as the temperature at which crystallization starts in i-PP for the cooling rate of 10 deg/min. For the calculations the value of K_g constant increased by 4% was used. The justification of these assumptions together with an estimation of the influence of possible errors in determination of the nucleation and the growth rate parameters on the predictions of i-PP conversion rate are discussed in details in Appendix II.

To predict the DSC curves for i-PP samples of thickness 280, 90 and 45 μm eq. (12) was used. The component in the conversion rate originating from spherulites nucleated on the sample surfaces was calculated based on eq. (14). The calculations were conducted for various values of nucleation density. It was assumed that the nucleation on the sample surfaces occurs at 130 °C, at the same temperature as the nucleation inside i-PP. The calculations were also conducted for an intense nucleation occurring on the sample surfaces at 135 °C.

RESULTS OF MODELING

In the Figs. 6—9 the predicted DSC curves are plotted for i-PP samples without and with spherulite nucleation on the sample surfaces of various density. The heat flow component in DSC signal originating from spherulites
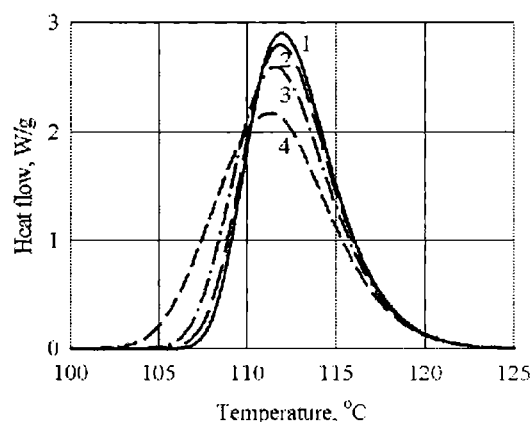

Fig. 6. Predicted DSC curves for crystallization without nucleation on the surfaces of i-PP samples of various thickness; 1 — infinite, 2 — 280 µm, 3 — 90 µm, 4 — 45 µm
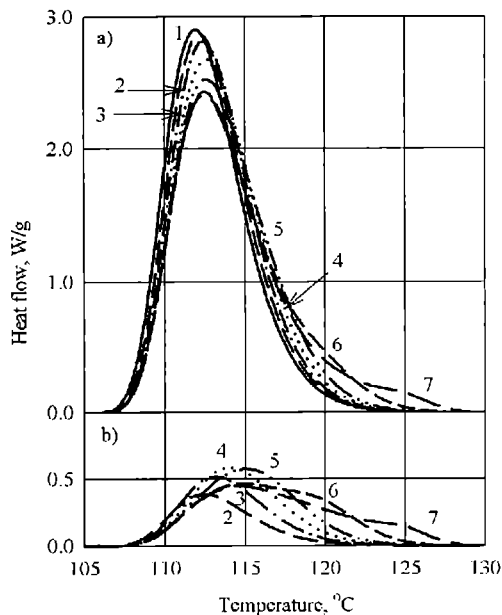
Fig. 7. Predicted DSC curves: a) total heat flow, b) component of heat flow originating from spherulites nucleated on the sample surfaces for crystallization of i-PP samples, 280 μm thick, with nucleation on the surfaces of various densities in μm⁻²: 1 — infinite, 2 — 1.6 · 10⁻⁴, 3 — 3.3 · 10⁻⁴, 4 — 6.6 · 10⁻⁴, 5 — 1.32 · 10⁻³, 6 — 6.35 · 10⁻³, 7 — 0.08
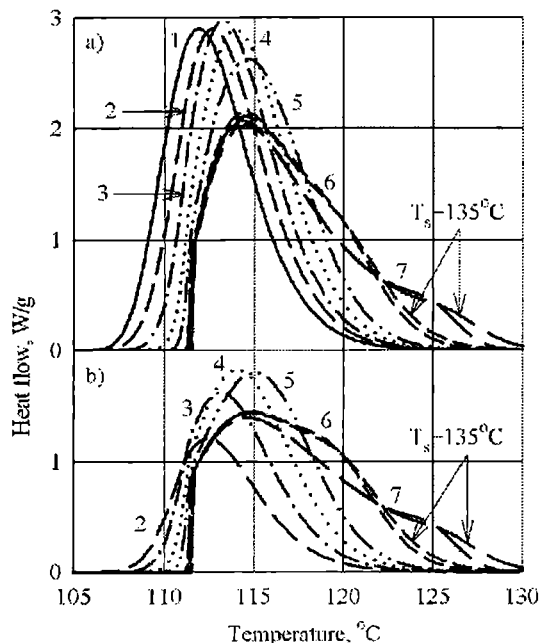

Fig. 8. Predicted DSC curves: a) total heat flow, b) component of heat flow originating from spherulites nucleated on the sample surfaces for crystallization of i-PP samples, 90 μm thick, with nucleation on the surfaces of various densities; curves denotations — see Fig. 7. Arrows indicate curves obtained assuming $T_s = 135$ °C.
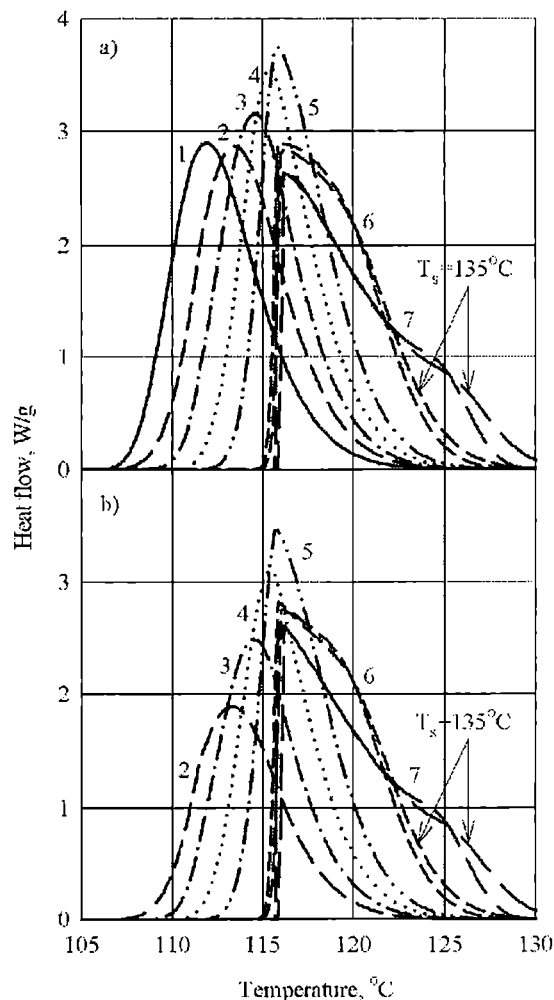

Fig. 9. Predicted DSC curves: a) total heat flow, b) component of heat flow originating from spherulites nucleated on the sample surfaces for crystallization of i-PP samples, 45 μm thick, with nucleation on the surfaces of various densities; curves denotations — see Fig. 7. Arrows indicate curves obtained assuming $T_s = 135$ °C.

nucleated on the sample surfaces is also drawn in Figs. 7—9. The maximum peak temperature and the total con-

tent of the spherulites nucleated on the sample surfaces against the nucleation density on the sample surfaces are plotted in Fig. 10.

In an absence of such nucleation (Fig. 6) the DSC curves broaden and their maxima shift slightly towards lower temperature with the decrease in the sample thickness. The nucleation on surfaces of 280 μm thick samples causes the elevation of the maximum temperature up to 0.7 deg and the lowering of the peak height up to 17% (Figs. 7 and 10). Very intense nucleation results in more significant rise of the curve at the beginning of crystallization. Very weak nucleation on the sample surfaces, below 10^{-4} μm⁻², does not cause any clear changes of the conversion rate curve with the decrease in sample thickness. However, for thinner samples the changes in the shape of the conversion rate curve and in the maximum positions with the increase in the nucleation density became more visible as it is demonstrated in Figs. 8—10.
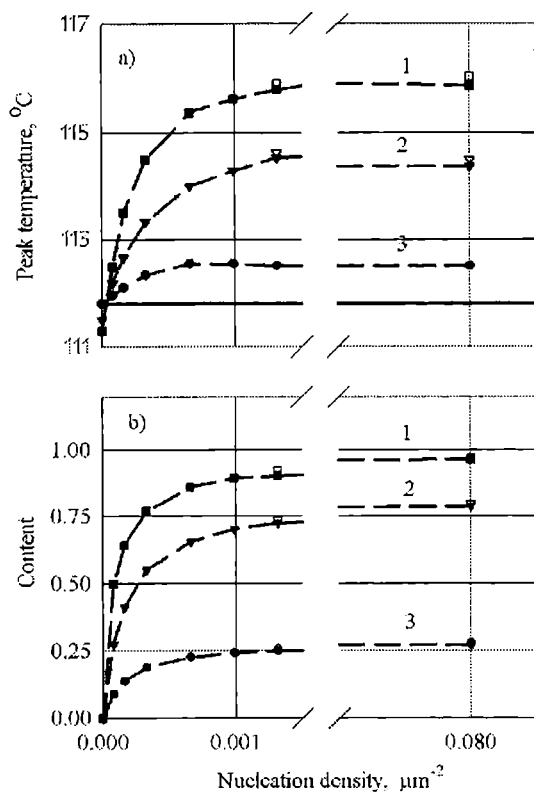
Fig. 10. Peak temperature (a) and the final content of spheru- lites nucleated on the sample surfaces (b) predicted by the model for i-PP samples of various thickness against density of spherulite nucleation on the sample surfaces: 1 — 45 μm, 2 — 90 μm, 3 — 280 μm; open symbols denote results obtained assuming $T_s = 135\ ^oC$ and solid line — infinite thickness

The maximum positions shift towards higher tempera- ture. With the increase in nucleation density the peak height initially increases but finally lowers for very in- tense nucleation. More intense nucleation results in ear- lier build-up of the conversion rate. For the nucleation density 0.00635 and 0.08 μm^{-2}, which corresponds to de- velopment of transcrystallinity, the shoulders on the high temperature slopes are seen. It is clear from Figs. 8—9 that this originates from the spherulites nucleated on the sample surfaces. With the increase in nucleation density the shoulder shifts to higher temperature. The conversion rate in thin samples with very intense nu- cleation on the surfaces falls down very fast after reach- ing the maximum value, which corresponds to the mo- ment when two transcrystalline fronts come in contact. Shifting the onset of nucleation on the sample surfaces to 135 °C does not produce any clear changes except for the insignificant elevation of maximum temperature and slightly earlier rise of the conversion rate in the case of 90 and 45 mm thick samples. That is because of a slow spherulite growth above 130 °C. On the contrary, the fast spherulite growth below 120 °C makes the conversion rate in transcrystalline samples very sensitive to sample thickness in that thickness range.

As it follows from Fig. 10, both the maximum tem- perature and the content of spherulites nucleated on the sample surfaces level off, with the increase in nu- cleation density on the sample surfaces, to the value leading to the development of transcrystallinity. The content of spherulites nucleated on the sample sur- faces reaches approximately 28, 80 and 97% in the samples of thickness of 280, 90 and 45 μm, respec- tively. For the 280 μm thick sample the above result allows to estimate the average thickness of the tran- scrystalline layer near the sample surface at approxi- mately 40 μm.

CONCLUSIONS

The results obtained indicate a significant role of nu- cleation on the sample surfaces on DSC measurements of crystallization kinetics of i-PP. Both the experimental re- sults and the model predictions demonstrate the change of shape of the conversion rate curve, the shift of maxi- mum temperature and the changes in the polymer spherulitic structure with the increase in nucleation den- sity and the decrease in the sample thickness. The strongest changes occur for the thinnest samples and a very intense nucleation on the surfaces leading to trans- crystallinity. However, even in the case of weaker nu- cleation not leading to transcrystallinity the shift in posi- tion of DSC peak was observed for thin samples. While the above described effects influence the heat flow distri- bution during crystallization, the entire heat crystal- lization remains the same within limits of experimental error.

The model predictions allow to explain the results of DSC measurements and spherulitic structure examina- tion. The predicted tendencies in the changes of DSC curves are similar to those measured experimentally. The tendencies in transformation of spherulitic pattern predicted theoretically are also observed. The thick transcrystalline layers are visible in 280 μm thick sam- ples while in the thinner samples those layers occupy nearly the entire volume of the sample. For weaker nu- cleation on the sample surfaces the content of spherulites nucleated on the sample surfaces is considerably smaller.

While the transcrystallinity manifests in earlier build- up of the conversion rate and in a change of DSC peak shape, the weak nucleation on the sample surfaces is more difficult to detect from DSC measurements and re- quires studies of sample morphology.

As it follows from the experimental data and the theoretical analysis, even weak spherulite nucleation on the sample surfaces influences the kinetics of crystal- lization, especially in thin samples of thickness ap- proaching the size of average spherulite. Although the present study and ref. [5, 6] are devoted to nonisother- mal crystallization one can expect similar effects during isothermal crystallization as well.

Thus, the sample surfaces are a potential source of error in the analysis of DSC data involving the classic Avrami or Ozawa methods. As it is demonstrated in the present paper, the crystallization kinetics is relatively weakly influenced by the surface nucleation and by the divergence from a true three-dimensional condition if the sample thickness exceeds several times the average spherulite size and the spherulite nucleation on the sample surfaces is not dense. In all other cases the use of Avrami or Ozawa type of DSC data analysis is erroneous.

On the contrary, a two-dimensional condition requires the sample thickness being at least several times smaller than the average spherulite size. Thus, the surface nucleation may dominate the crystallization kinetics and screen entirely the bulk polymer nucleation.

APPENDIX I

We have to note that in an instantaneously nucleated spherulitic sample if the growth rate changes uniformly within the whole sample, the ratios between all characteristic distances are constant [11], independently on the growth rate time dependence. The ratio of the average radius (R_s) [determined from the average area visible in cross-section (S) as $R_s = (S/\pi)^{1/2}$] over the average spherulite radius (defined as $R_{av} = (3V/4\pi)^{1/3}$, where V denotes the volume of the average spherulite) is also a constant:

$$\frac{R_s}{R_{av}} = c \qquad (1A)$$

Thus, the density of nucleation (D) can be calculated from the formula:

$$D = \frac{3}{4}\left(cS^{-\frac{1}{2}}\right)^3 \pi^{\frac{1}{2}} \qquad (2A)$$

To find the value of R_s/R_{av} a spherulitic structure was computer simulated. 10 000 spherulite centers were generated by means of pseudorandom number generator in a cube of 200×200×200 of arbitrary units. Further calculations were conducted for a series of planes crosssecting the cube to find spherulites crossed by those planes. On each plane the regular network of points in distances of 0.25 unit was chosen. If spherulites are nucleated instantaneously, every sample point is occluded by a spherulite growing from the closest primary nuclei. Thus, for each point the closest spherulite center was determined. The average spherulite cross-section S was calculated by dividing the cross-section surface area by the number of spherulites passing those cross-sections, which enabled us to find the value of R_s/R_{av} equal to 0.756.

Based on this value and the value of S equal to 3400 μm^2 the density of primary nucleation was calculated as $2.9 \cdot 10^{-6} \mu m^{-3}$.

APPENDIX II

For the prediction of crystallization kinetics in i-PP (Rapra) sample during uniform cooling at a rate 10 deg/min the eq. (12) was used. The H and H_s functions were assumed equal to zero in order to calculate the crystallization rate in a sample, which is thick enough to neglect the effect of boundaries. The spherulite growth rate temperature dependence in the form of eq. (15) was used and instantaneous nucleation with the density $2.9 \cdot 10^{-6} \mu m^{-3}$ occurring at 130 °C was assumed. The conversion rate was multiplied by the heat of crystallization of i-PP — 106 J/g.

DSC curves recorded for 280 μm thick i-PP samples crystallizing in contact with the other material changed very little independent of the type of the material, except the case when nucleation on the surfaces was very intense. Thus, DSC curve obtained for 280 μm thick sample in contact with DSC pan was used as a reference. To estimate the influence of the possible errors made in the determination of parameters describing both the nucleation and the growth rate, the following cases were considered:
— decrease in nucleation density,
— decrease in onset of crystallization,
— shift of the growth rate temperature dependence with a respect to temperature,
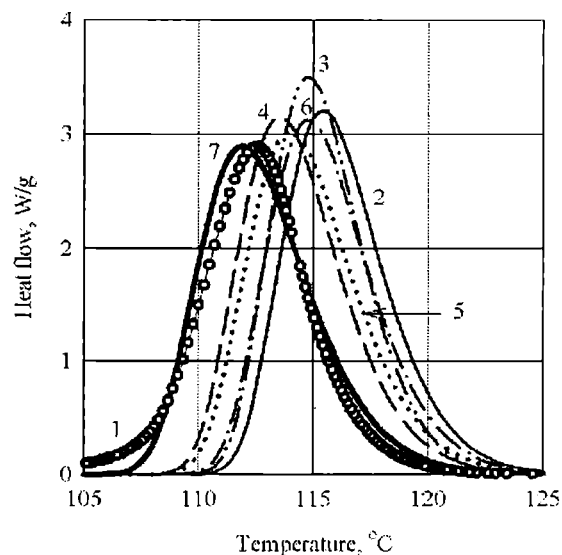— changes in G_0 and K_g constants.

Fig. 11. DSC curves: 1 — experimental; predicted by the model for crystallization of i-PP samples of infinite thickness for different modifications of parameters describing the spherulite nucleation and the growth rate: 2 — initial, 3 — $T_i = 125$ °C, 4 — $T + 2$ deg, 5 — $D/2$, 6 — $G_0 \cdot 0.9$, 7 — $K_g \cdot 1.04$

The exemplary results are plotted in Fig. 11 together with the experimental peak. As it is seen, the theoreti-

cally predicted peaks were narrower and positioned at a higher temperature than the experimental one. The decrease in temperature of the crystallization onset to 125 °C moved slightly the theoretical peak to lower temperature but resulted also in its narrowing. The displacement of the curve towards the lower temperature caused by the shift of the growth rate dependence with a respect to temperature in eq. (15) by 2 deg was also non sufficient to fit the theoretical curve to the experimental one. Inadequate change in the position of the peak was also obtained by the decreasing in the nucleation density by a half and G_0 constant to 0.9 of its initial value. One has to consider that the changes introduced to the parameters describing the nucleation and the growth rate were at the limits or even beyond the limits of acceptable experimental errors. On the contrary the increase in K_g constant by 4% only resulted in a good fit to the experimental data. Therefore in further calculations such value of K_g with other parameters unchanged are used.

REFERENCES

1. Billon N., Haudin J. M.: *Colloid Polym. Sci.* 1989, **267**, 1064.
2. Billon N., Magnet C., Haudin J. M., Lefebvre D.: *Colloid Polym. Sci.* 1994, **272**, 633.
3. Piorkowska E.: *Colloid Polym. Sci.* 1997, **275**, 1035.
4. Piorkowska E.: *Colloid Polym. Sci.* 1997, **275**, 1046.
5. Billon N., Henaff V., Pelous E. Haudin J. M.: *J. Appl. Polym. Sci.* 2002, **86**, 725.
6. Billon N., Henaff V., Haudin J. M.: *J. Appl. Polym. Sci.* 2002, **86**, 734.
7. Bartczak Z., Galeski A., Krasnikova N. P.: *Polymer* 1987, **28**, 1627.
8. Martuscelli E., Silvestre C., Abate G.: *Polymer* 1982, **23**, 229.
9. Cark E. J., Hoffman J. D.: *Macromolecules* 1984, **17**, 878.
10. Piorkowska E.: *J. Chem. Phys.* 1995, **99**, 14 016.
11. Piorkowska E.: *J. Chem. Phys.* 1995, **99**, 14 024.